Near-Field Nanomodification of Thin Films Using Femtosecond Laser and Atomic Force Microscope

A. Chimmalgi, T. Y. Choi, C. P. Grigoropoulos, D. Wan, and K. Komvopoulos
Department of Mechanical Engineering, University of California, Berkeley, CA 94720

ABSTRACT

Ultra-short pulsed laser radiation has emerged as a powerful and effective tool for high-precision material processing and surface micromodification. Apertureless film surface nanomodification was accomplished through enhancement of the near field of a surface force microscope (SPM) probe tip by irradiation with femtosecond laser pulses. Simulation results for the spatial distribution of the laser field intensity under the tip neighborhood based on the finite difference time domain method are presented along with surface nanomodification results for various thin films using a 800 nm Ti-Sapphire femtosecond laser system coupled with a commercial SPM in ambient air. High spatial resolution (~10-12 nm), wide range of substrate materials, ability to machine complex nanopatterns, and possibility of massive integration of microprobe tips make this method an effective nanofabrication tool. Potential nanotechnology-related applications include lithography, photonics, ultra-high density data storage, and various biofluidics.

Keywords: surface nanomodification, scanning probe microscopy, femtosecond laser irradiation, near-field enhancement.

1 INTRODUCTION

Nanostructures exhibiting dimensions difficult to achieve with conventional optical lithography techniques are finding ever-increasing applications in various emerging fields. However, ultra-high resolution, reliability and throughput fabrication of these nanostructures is essential if applications incorporating nanodevices are to gain widespread acceptance. Due to the light diffraction that limits the size of the minimum resolvable feature to one-half of the wavelength, conventional optical lithography does not enable surface modification at the nanoscale. Hence, novel lithography techniques, such as electron- and ion-beam and x-ray lithography, have attracted the attention of researchers in recent years. However, large capital cost, slow processing speed, lack of suitable materials for fabricating various optical elements, and radiation hazards make these processes less desirable. Scanning probe lithography techniques are being explored as a plausible alternative [1]. In addition to providing a means for three-dimensional atomic resolution surface imaging and measurement of various surface properties, scanning probes have been used in various high-resolution nanostructuring studies and also to manipulate and position single atoms, thereby serving as an all-inclusive nanofabrication tool.

Nanostructuring of various materials including Au, Au/Pd, PMMA, and PC has been accomplished by illuminating a scanning probe microscope (SPM) tip with nanosecond laser pulses [2-9]. Despite the high resolution (~30 nm) reported for laser nanoprocessing schemes involving scanning tunneling microscopy (STM) [3,4,8,10], this method is unsuitable for biotechnology applications due to restrictions on the electrical conductivity of the processed materials and scanning probe tip and the ambient working conditions. Nanofeatures of lateral dimensions less than 20 nm obtained with AFM operated in the contact and non-contact modes [2,6,7] suggest that this method provides an alternative means for overcoming the previous obstacles. However, very little is known about the actual processing mechanism in AFM-based nanomodification schemes. In most cases, either AFM or STM contact mode configurations were employed with the tip in actual contact or in the very close proximity with the sample, thereby complicating the actual underlying modification mechanism. Although high enhancement factors for the electric field intensity in the vicinity of the tip have been proposed [5,6], the reported mechanical contact between the tip and the sample surface due to the thermal expansion [9,10] complicates the study of the effect of process parameters. To the best of the authors' knowledge, no reports of experimental results have been published in the literature wherein the tip-sample separation was controlled and varied accurately during surface modification.

In this study, the surfaces of thin films of Au, In, and amorphous silicon (a-Si) were modified by illuminating a standard Si AFM probe tip with ultra-fast laser pulses to produce a profound near-field enhancement effect. The different nanopatterns, such as multiple line grids, craters, hillocks, and contours, and the stability of the obtained nanofeatures (confirmed by scanning again the processed areas after several hours) illustrate the feasibility of this nanomodification scheme. Results are presented to elucidate the dependence of apparent crater depth on laser fluence and tip-sample separation distance along with simulation results for the electric field intensity distribution in the proximity of the AFM probe tip. The predicted

intensity distributions are shown to be in good agreement with experimental results for the observed feature size. Possible applications of this processing scheme are discussed in the context of the presented results.

2 EXPERIMENTAL APPROACH

A schematic diagram of the experimental apparatus is shown in Fig. 1. Femtosecond pulses of 83 fs full width half maximum (FWHM) duration and wavelength $\lambda = 800$ nm with pulse energies in the range of 125 nJ–3.7 μJ were used in the present experiments.

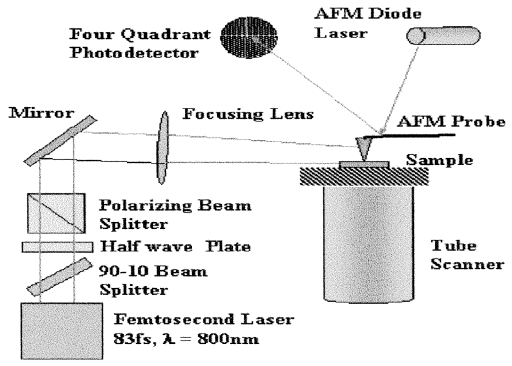

Figure 1: Schematic diagram of the experimental setup.

A two-step attenuation scheme was used to accurately control the pulse energy, wherein 10% of the transmitted laser beam from the beam splitter was further attenuated using a half-wave plate and polarizing beam-splitter combination. The polarizing beam splitter transmits P-polarization component used for nanomodification. The beam was then focused on the AFM probe tip using a 175 mm positive lens, giving a $1/e^2$ beam spot diameter of ~74 μm, as measured by the knife-edge technique. Laser alignment was achieved by simultaneously viewing the tip from the top and the side using combinations of 12X zoom lens, 10X long focal length objective, and high-sensitivity CCD camera. The laser beam was aligned at a grazing angle of incidence to the sample surface.

A multi-mode AFM (Digital Instruments) was operated in the contact mode for imaging purposes with typical scanning parameters. While performing surface nanomodification in combination with the laser beam, a constant tip-sample separation was maintained by using a commercial nanolithography software (Digital Instruments) that disables the tip position feedback signals and enables traversing the tip along complex contours. Commercially available, contact mode, etched Si microprobes possessing tips with an apex radius of curvature equal to 5-10 nm were used to modify the sample surfaces. Thin films of ~25-nm-thick Au, ~50-nm-thick a-Si, 15-nm-thick Au deposited over a 10-nm-thick Cr (henceforth be referred to as Au/Cr film), and In were used in this study. All the films were deposited on Si(100) substrates, except for the a-Si film that was deposited on quartz samples. Damage of the AFM tips was not observed even after hundreds of thousands of laser pulses.

3 RESULTS AND DISCUSSION

In this section, simulation results for the enhancement of the electric field in the tip/sample gap are presented first, followed by experimental nanomodification results for different film materials illustrating the feasibility of the present scheme.

3.1 Numerical Results

Electric field intensity distributions were obtained using the finite difference time domain technique and near-field simulation software. Numerical results are presented for $\lambda = 800$ nm (near-IR fundamental harmonic). A full three-dimensional simulation was performed that involved solving the four Maxwell's equations and two constitutive relations simultaneously with the current relation. Leapfrog technique was used to discretize the time variable, which involved solving the electric fields E at integer time steps while the magnetic fields H were evaluated at integer plus one-half time steps.

The tip profile was constructed using cylindrical nodal elements of progressively larger radii at increased depth from the apex. A hemispherical node was placed at the tip apex with a radius of 5.4 nm, closely approximating the dimensions of the actual probe tip. Figure 2 shows the electric field intensity distribution for λ =800 nm, incident wave of unit E-field amplitude, P-state of incident polarization (parallel polarization) at grazing angles of incidence, Si probe tip, and a-Si sample surface. A profound increase of the electric field intensity is shown in the tip/sample surface gap.

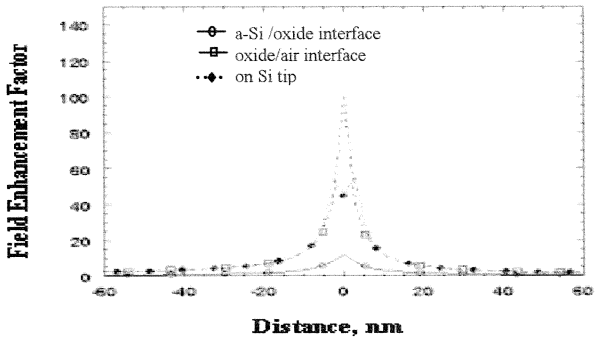

Figure 2: Normalized electric field intensity distribution under a Si tip irradiated with incident laser ($\lambda = 800$ nm) and a-Si sample surface.

The electric field distribution at the tip exhibits the "antenna effect," reported to be predominant at longer wavelengths [12]. The lateral confinement of the field is believed to be the main factor responsible for the high spatial resolution modification observed experimentally. The effect of a native oxide layer is quite evident since the net intensity at the a-Si/oxide interface is greatly reduced. At the oxide/air interface, the obtained high enhancement factor of ~100 may be responsible for the observed convex nanostructures. Nevertheless, these enhancement values are theoretical estimations. The actual enhancement strength may differ due to several influencing factors, such as increase of the effective tip-sample separation distance during nanomodification resulting from material removal, approximations involved in the modeling of the actual tip shape and sample size, presence of any surface oxides, in-situ change of the tip apex radius due to using the same tip for both imaging and surface modification.

3.2 Experimental Results

The laser pulse energy and tip-sample surface separation distance were found to strongly affect the dimensions of the features produced on Au film surfaces. The lateral dimensions and depth of surface features increased linearly with pulse energy [11]. A threshold value was determined at ~500 nJ of input laser pulse energy (i.e., ~0.012 J/cm^2 of laser fluence) for which the depth of the produced feature was almost comparable to the Au film surface roughness. Wider and deeper features were produced by successively increasing the pulse energy. To produce continuous line features, the laser was operated at 1 kHz for ~2 s, while the sample was scanned at a speed of 1 μm/s. For laser operation at 0.5 kHz for 2 s and input laser fluence of ~0.1 J/cm^2, increasing the tip-sample separation distance resulted in shallower surface craters. These results confirmed that the laser fluence and tip-sample separation distance could be adjusted to precisely control the feature dimensions. The minimum feature size obtained in these nanomodification experiments was less than ~10 nm in lateral dimensions, and the maximum crater depth produced with multiple laser pulses was ~10.5 nm.

Figure 3 shows nanoprocessing results for laser fluence equal to 0.069 J/cm^2, demonstrating the flexibility offered by the present nanomodification scheme. Linear scanning speeds of 20 μm/s and tip-sample separation distance in the range of 3-5 nm were used, making the entire processing sequence considerably fast. It is evident from Fig. 3 that the present technique can be used to make both negative and positive templates for subsequent use in mass production of nanostructures.

Figures 4(a) and 4(c) show formation of nanocraters on Au/Cr and In film surfaces for laser fluence equal to 0.017 and 0.035 J/cm^2, respectively. The corresponding profiles shown in Figs. 4(b) and 4(d) provide information about the dimensions of the produced craters.

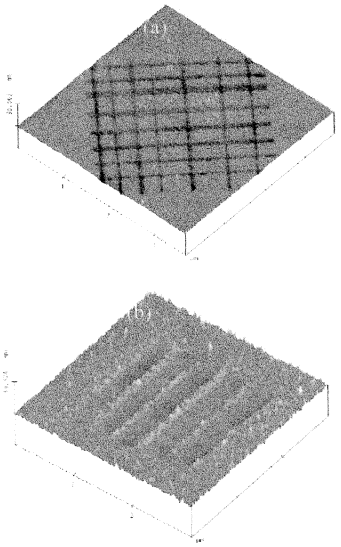

Figure 3: AFM images showing arrays of precisely spaced line marks on (a) ~25 nm and (b) ~15 nm thick Au films on Si(100) substrates.

The depth of the craters shown in Figs. 4(a) and 4(b) is about 17.5 and 10 nm, respectively, which is larger than the Au and In film thickness. Thus, very small areas of underlying material (Cr and Si, respectively) were exposed at the bottom of each crater. This opens up the possibility for a number of applications requiring selective surface patterning and functionalization and the fabrication of nanophotonic devices.

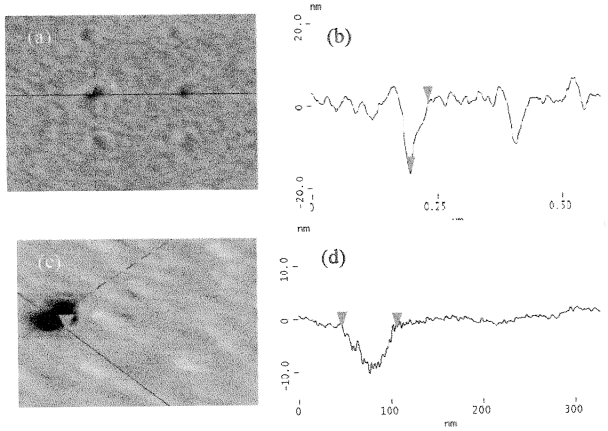

Figure 4: AFM images showing nano-crater formation on (a) 15 nm Au/10 nm Cr and (b) 8 nm In films on Si(100) substrates. The corresponding surface profiles in (b) and (d) illustrate that the craters are through the Au and In films, exposing Si surface nanodomains.

Elevated convex structures were produced while performing nanomodification of a-Si and Au/Cr films. Subsequent nanomachining using fluences of ~0.035 J/cm^2 resulted in formation of craters as deep as ~49 nm. Figure 5(a) shows the controllable elevated convex nanostructures processed by this scheme. Figure 5(b) shows the formation of such nanostructure on the Au/Cr two-layer film surface. In a subsequent scan, the tip was held above the center of the hillock at a tip-sample separation distance of 4 nm and pulsed with laser at 1 kHz for 5s. It was possible to drill through the hillock, producing a ~49 nm deep crater (Fig. 5(c)). It was observed that the overall shape of the hillock changed considerably (Fig. 5(d)). A principal objective of work in progress is to shed light into the underlying fabrication mechanism leading to the development of these nanostructures through numerical simulations and microscale ablation of thin films with a tightly focused laser beam, using long working distance objective lenses.

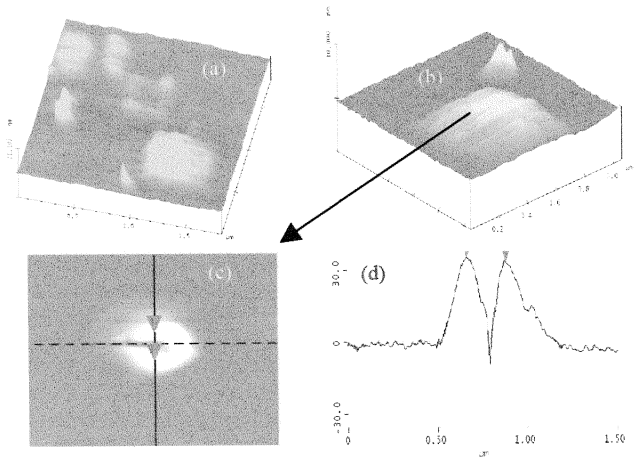

Figure 5: AFM images showing (a) nanostructuring of a-Si thin films to form controllable hillocks with ~0.035 J/cm^2 fluence, (b) hillock formation on Au/Cr two-layer film, and (c) drilling through hillock by centering the AFM tip over the center of the hillock and illuminating it with ~0.035 J/cm^2 fluence of laser pulses of 1 kHz for 5 s. The surface profile in (d) shows the cross-section area of the modified hillock.

The possibility of utilizing multi-arrays of AFM probe tips with integrated actuator and sensor mechanisms to increase the overall throughput of the process makes the present nanomodification scheme highly attractive. Several possible applications are envisioned in leading-edge nanotechnology areas, such as high-resolution lithography, controlled deposition and machining of various material surfaces, ultra high-density data storage, electronics, photonics, and biotechnology applications, specifically biofluidics and multi-assay biochips.

4 CONCLUSIONS

High spatial resolution nanostructuring of various thin films was accomplished with great accuracy and reproducibility by focusing femtosecond laser pulses onto an AFM probe tip placed in the proximity of different film surfaces. Processing of nanostructures possessing lateral resolution of ~10 nm was demostrated. Simulations of the electric field intensity accurately predict the high spatial resolution observed experimentally and support the proposition that the enhancement of the electric field in the probe proximity is a key factor in this nanomodification process. Different complex nanopatterns were produced to demonstrate the flexibility of the surface nanomodification scheme. The results of this study indicate that coupling of femtosecond pulsed lasers with surface microprobes provides an effective and versatile processing scheme for surface nanomodification involving deposition, machining, and restructuring. Simultaneous illumination of multi-arrays of microprobe tips by ultra-short laser pulses of different fluence would increase the throughput effectiveness of the present nanomodification process.

ACKNOWLEDGMENTS

This research was funded by the National Science Foundation under Grant No. CTS-0103390.

REFERENCES

[1] C. F. Quate, Surf. Sci. 386, 259, 1997.

[2] J. Jersch, F. Demming and K. Dickmann, Appl. Phys. A 64, 29, 1997.

[3] A. A. Gorbunov and W. Pompe, Phys. Stat. Solidi. A 145, 333, 1994.

[4] J. Jersch and K. Dickmann, Appl. Phys. Lett. 68, 868, 1996.

[5] K. Dickmann, J. Jersch and F. Demming, Surf. Int. Anal. 25, 500, 1997.

[6] Y. F. Lu, B. Hu, Z. H. Mai, W. J. Wang, W. K. Chim and T. C. Chong, Jpn. J. Appl. Phys. 40, 4395, 2001.

[7] S. M. Huang, M. H. Hong, Y. F. Lu, B. S. Lukyanchuk, W. D. Song and T. C. Chong, Appl. Phys. 91, 3268, 2002.

[8] Y. F. Lu, Z. H. Mai, G. Qiu and W. K. Chim, Appl. Phys. Lett. 75, 2359, 1999.

[9] R. Huber, M. Koch and J. Feldmann, Appl. Phys. Lett. 73, 2521, 1998.

[10] J. Boneberg, H.J. Munzer, M. Tresp, M. Ochmann and P. Leiderer, Appl. Phys. A. 67, 381, 1998.

[11] A. Chimmalgi, T. Y. Choi, C. P. Grigoropoulos and K. Komvopoulos, Appl. Phys. Lett., 2003, submitted.